Bulgarian Journal of Physics vol. **49** (2022) 399–409

A Simple Chemical Route for Synthesis of Microsphere of Stannous Oxide at Room Temperature

Sandeep A. Arote, **Dipak L. Gapale**, **Prashant K. Baviskar**, **Pranav P. Bardapurkar**, **Sanjaykumar N. Dalvi**, **Sainath R. Navale**, **Balasaheb M. Palve***

Department of Physics, Sangamner Nagarpalika Arts, D.J. Malpani Commerce and B.N. Sarda Science College (Autonomous), Sangamner, Dist-Ahmednagar-422605, India
*Corresponding author E-mail: palve@sangamnercollege.edu.in

Received *25 February 2022*, Revised *24 September 2022*

doi: https://doi.org/10.55318/bgjp.2022.49.4.399

Abstract. The microspheres of stannous oxide were synthesized via simple room temperature wet chemical route using potassium hydroxide (KOH) as the precipitating agent. The prepared samples were characterized by the X-ray diffractometry (XRD), Scanning electron microscopy (SEM), and Photoluminescence and Ultraviolet-visible spectroscopy. The structural, optical and morphological properties of synthesized samples were controlled by varying the concentration of precipitating agent. It was observed that, the concentration of KOH affected the sample morphology and phase also. XRD study showed the change in phase from stannic oxide (SnO_2) to stannous oxide (SnO), with increase in KOH concentration. SEM micrograph showed the change in morphology from nanoparticle network to the porous microsphere as an effect of variation of KOH concentration. TEM confirm the formation of flower like morphology by interconnection of nanosheets having <200 nm in size. In this study, the size of individual SnO microsphere was controlled in the range of 10–14 μm in diameter, suitable for various photocatalytic and sensing applications.

KEY WORDS: Wet chemical route; stannous oxide; microspheres; cross-linked nanosheets; size-controlled synthesis.

1 Introduction

It has been extensively investigated that, self-assembled ordered semiconducting nanostructures exhibited enormous effect on device performance including sensors and optoelectronic devices [1–3]. This is due to the fact that, properties of nanostructures depend on synthesis method, size, shape and composition. The

three dimensional (3D) nanostructures offer huge surface to volume ratio, enhanced surface reactivity, microstructural, optical and electrical properties [3,4]. In the modern era, search or development of synthesis method that has an ability to reduce the size of the nanocrystals and control their shape is one of the major challenge of scientific community [4]. Stannous oxide (SnO) is p type wide band gap (bulk band gap of ~2.8 eV) semiconducting material [5, 6] and a promising candidate for photocatalyst [7], photoluminescence [8], sensor [9] and field-effect transistor [10] applications. The advanced photocatalysts and sensor technologies require well crystallized nanocrystals with high surface area, porous and uniform size distribution [11]. A large number of reports on synthesis of SnO nanoparticles, nanosheets, nanobelts, nanowhiskers and nanowires using advanced / modified chemical or physical methods are available in the literature [7–13]. However, it still remains a promising task for researcher to obtain pure SnO nanocrystals in large quantity at room temperature and to minimize unwanted by-products. Further, there are very few reports on synthesis of porous three dimensional micro/nanostructured SnO. Recently, Haspulat *et al.* reported SnO nanocrystals composed of pentagonal, rod and plate shapes [14]. They observed that the SnO nanosheets with high specific surface area and higher UV absorbance have excellent photocatalytic activity for highly polluting organic dyes. We have also reported the chemically prepared SnO_2 for nanostructured solar cell application [15, 16]. However, these porous nanosheets were overlapped due to the planar geometry and consequently have decreased surface area. The cross-linked orientation of nanosheets to form three dimensional architecture may enhance the effective surface area and hence its reactivity. Recently we have reported the effect of NaOH for the synthesis of SnO and SnO_2 [17].

Present work reports structural and optical investigations of SnO microspheres with cross-linked nanosheets synthesized at low temperature using in-situ wet chemical method. This approach would be economic, fast and modest synthesis route.

2 Experimental

2.1 Material

The precursors were analytical grade stannous chloride (dihydrate, $SnCl_2 2H_2O$) and anhydrous potassium hydroxide (KOH) obtained from LOBA chemicals.

2.2 Synthesis of SnO and SnO_2

The synthesis approach was based on precipitating agent assisted wet chemical method. 1.4 gm amount of stannous chloride was dissolved in double distilled water and then added into a glass vessel containing KOH solution of particular concentration. The reaction was maintained under continuous vigorous mag-

netic stirring at room temperature (27°C) for 15 min. On completion of the reaction, the precipitates were collected, washed with distilled water and absolute ethanol for several times and dried over the night. Above procedure was repeated twice by varying the KOH concentration. The concentration of KOH solution was adjusted to assure the alkaline environment during each reaction. A gray precipitate was obtained on addition of 2M KOH solutions to stannous chloride, which suddenly changed to white crystals on stirring the mixture for a few minutes. Further, when 4M KOH solution was added to stannous chloride and stirred continuously, the initial gray precipitate turned to light yellow and then quickly to black colored crystals. In order to study the effect of annealing, the as prepared samples were annealed at 450°C for one hr. The samples with 2M KOH were termed as S1 and S2, that with 4M KOH, as S3 and S4 before and after annealing, respectively.

2.3 Physicochemical characterization

The structural properties were studied using an X-ray diffractometer (XRD, Rigaku D/B max-2400 with Cu-Kα radiation, $\lambda = 1.54$ Å). Optical absorption spectra of the prepared samples were recorded using JascoV-670 spectrophotometer in the range of 200 to 800 nm. The microstructure and morphological topographies were observed using SEM (JEOL-JSM 6360-A). Photoluminescence emission (PL) properties were studied using Perkin Elmer LS55 with excitation wavelength of 320 nm.

3 Results and Discussion

3.1 Structural properties

The structural properties of the samples were analyzed using X-ray diffractometry before and after annealing. Figures 1 and 2 show X-ray diffractograms for all the four samples (S1, S2, S3 and S4), which confirm the successful synthesis of SnO_2 and SnO nanocrystals at room temperature. The samples annealed at 450°C in both experiments (S2 and S4) show increase in peak intensity, which can be attributed to enhancement in crystallinity of the samples. However, crystallite size is not affected due to annealing, as the broadening of peaks appears to be same. From the XRD results (Figure 1), it can be clearly understood that the samples S1 and S2 are composed of SnO_2 phase with tetragonal rutile crystal structure (JCPDS card no. 41-1445), which belongs the space group $P4_2/mnm$. In sample S1, prepared with 2M KOH at room temperature, some impurity peaks were observed at 28.5°, 30° and 31.1° which may be due to the existence of some impurities in the sample.

Figure 2**a** shows the diffractograms for the samples prepared with 4M KOH. All the peaks in these diffractograms correspond to pure tetragonal phase of SnO

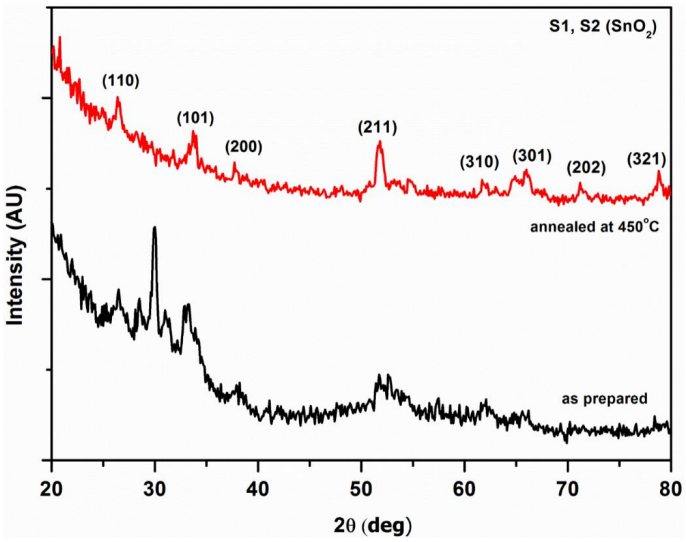

Figure 1. XRD pattern of as prepared and annealed samples with 2M KOH.

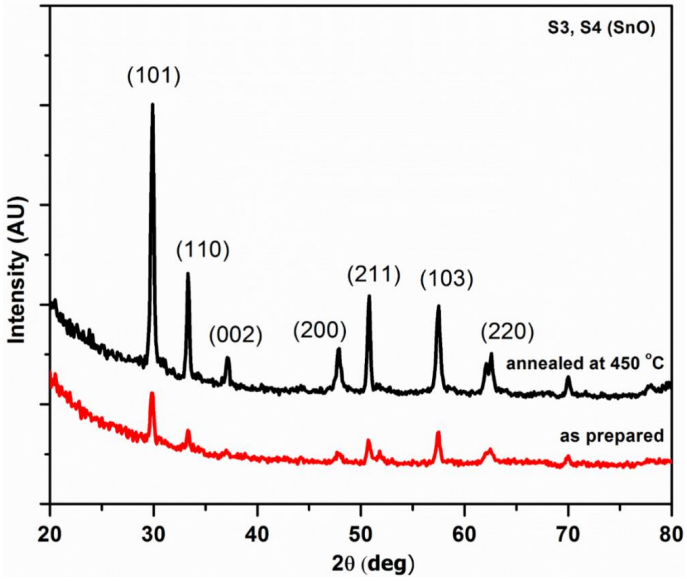

Figure 2. (a) XRD pattern of as prepared and annealed samples with 4M KOH.

(JCPDS No. 06-0395, space group: P4/mnm, unit cell parameters: $a = b = 3.80$, $c = 4.83$ Å) without any impurity peaks. The peak positions are extracted by curve fitting using Gaussian standard deviation method. Gaussian fitting of

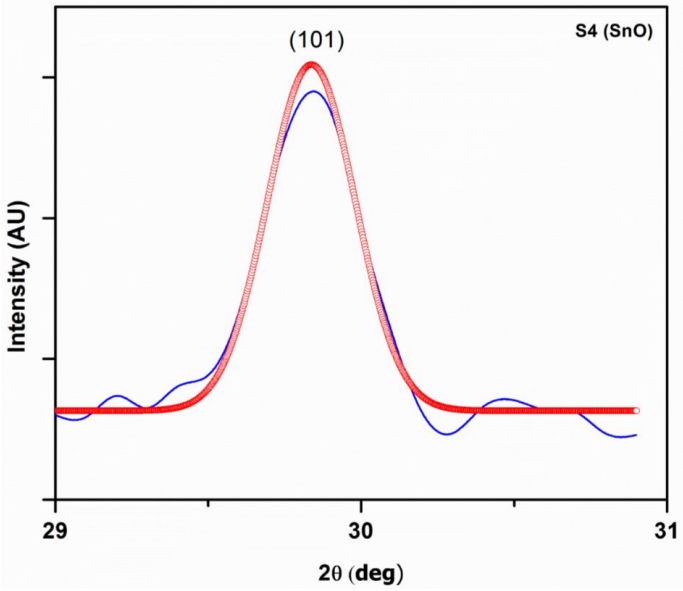

Figure 2. (b) Gaussian fitting of prominent peak of (101) plane of annealed samples with 4M KOH.

prominent peak for (101) plane is shown in Figure 2**b**. The peak positions obtained after Gaussian fitting is 29.83 for (101) plane, which is most accurate.

It has been reported in the literature that the nanostructured materials prepared by chemical routes may contain certain impurities. The presence of impurities in sample S1 indicates in complete conversion of reactants in desired product [18, 19].

3.2 Microstructural properties

3.2.1 Scanning electron microscopy

Figure 3 shows the SEM images of all synthesized samples at different concentration of KOH. It is observed that the KOH concentration has considerable influence on surface morphology of samples. The 2M KOH resulted in the formation of SnO_2 nanoparticles network with an average diameter of 300 nm. The SEM images of synthesized sample using 4M KOH shows formation of 3D porous SnO microspheres with an average diameter of about 12 μm. Magnified SEM image shows that the microspheres are composed of 2D inter-linked nanosheets and are self-assembled to form flower like structures. Such an interlinked nanostructures also forms 3 dimensional macro-porous network which may help to enhance the sensing and photo-catalytic activity. Further, no re-

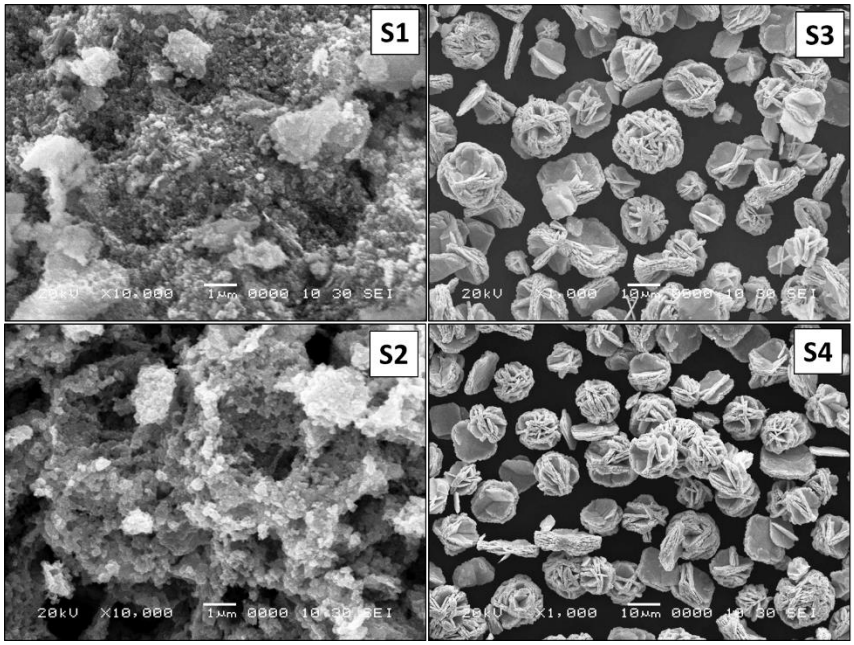

Figure 3. SEM micrographs for as-synthesized SnO_2 (S1) & SnO (S3) and annealed SnO_2 (S2) & SnO (S4) nanostructures.

markable change in morphology was observed even after annealing at 450°C which indicates that, the microspheres are not just aggregated structures but are the self-assembled ones.

3.3 Transmission electron microscopy

The crystallinity and morphology of nanostructured SnO sample was analyzed using transmission electron microscopy (TEM) technique. Figure 4 shows TEM micrograph and selected area electron diffraction (SAED) for SnO (S3) sample. From TEM image (Figure 4**a**) 2D nanosheets having size up to 200 nm with few nm thickness are observed and the SAED pattern shown in Figure 4**b** reveals the polycrystalline nature of the SnO nanostructure.

3.4 Optical properties

The optical absorption spectra for annealed samples (S2 and S4) were recorded in the range of 200 to 800 nm in diffused reflectance mode with equal quantity of the powder samples. As in shown in Figure 5**a**, the absorption spectra for both the samples have a narrow peak near the band edge with λ_{max} at 271 nm and 300 nm for the samples S2 and S4 respectively. Fano like shape is observed

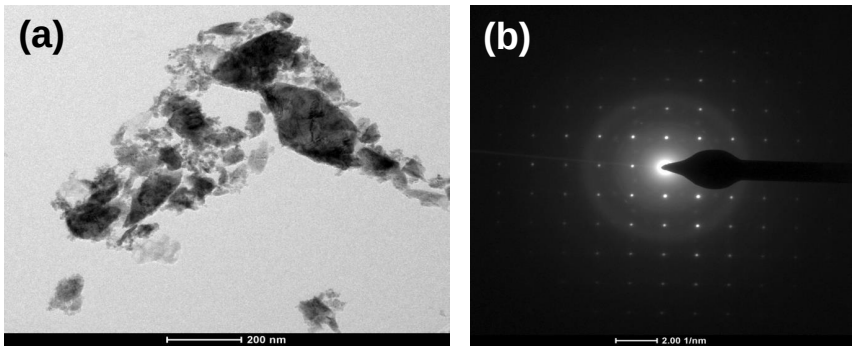

Figure 4. **(a)** Low magnification bright field image; and **(b)** SAED pattern of as synthesized SnO (S3) nanostructure.

in SnO absorption spectra may be due to the less defect concentration. The optical band gap energies for these samples are estimated using the absorption spectrum fitting (ASF) method by plotting (absorbance/λ)^2 vs. 1/(λ (nm)) curve (Figure 5**b**) [20]. Using ASF, the value of energy band gap can be calculated using

$$E_g^{\mathrm{ASF}} = \frac{1240}{\lambda_g} \ ,$$

where E_g^{ASF} is the band gap energy calculated using ASF method with λ_g as the corresponding wavelength calculated by extrapolating the (absorbance/λ)^2 vs. 1/λ curve. From Figure 5**b**, for S2 sample, i.e. SnO_2, the band gap energy E_g^{ASF} is about 3.43 eV. Similarly the calculated E_g^{ASF} for S4 sample, i.e SnO microphores, is about 2.89 eV and are consistent with previous reports on SnO and SnO_2 [22, 23]. According to literature, band gap energy of SnO varies from 2.7 to 3.4 eV as an effect of preparative and structural parameters [5, 21]. The observed increase in E_g for both the samples can be attributed to quantum

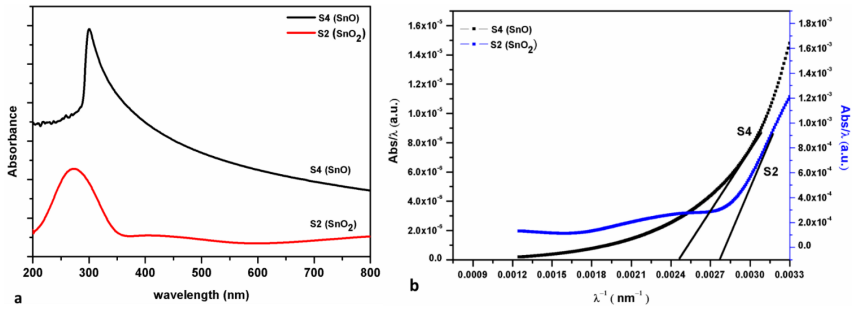

Figure 5. **(a)** Optical absorption spectra; and **(b)** band gap energy calculation of annealed samples (S2 and S4).

confinement effect [17, 19–23].

3.5 Photoluminescence (PL) properties

Figure 6 shows the room-temperature PL spectra for S2 and S4 samples, obtained at excitation wavelength of 320 nm. A strong emission peak observed in Figure 6**a** for sample S2 (i.e. for SnO_2) at 345 nm (3.6 eV) corresponds to the near band-edge emission [24]. The other emission peaks obtained at higher values of wavelength may correspond to defects in the samples, like structural defects, defects in nanostructures, luminescent centers etc [25–27]. The broad and less intense peak appeared at 482 nm can be assigned to the oxygen vacancies, that creates the defect levels in the neighborhood of conduction band [28, 29].

Figure 6**b** shows PL spectra for SnO microspheres, recorded for sample S4. The spectra shows a strong emission peak at 386 nm (3.21 eV) which can be attributed to the near band edge emission [30, 31], whereas, the peaks at 412 nm and 474 nm are accredited to the defects in the material [32]. According to the study performed by Togo *et. al.*, the p-type conductivity of SnO originates from Sn vacancies [21]. Thus, the emission peak observed at about 474 nm is ascribed to the Sn vacancies in the sample.

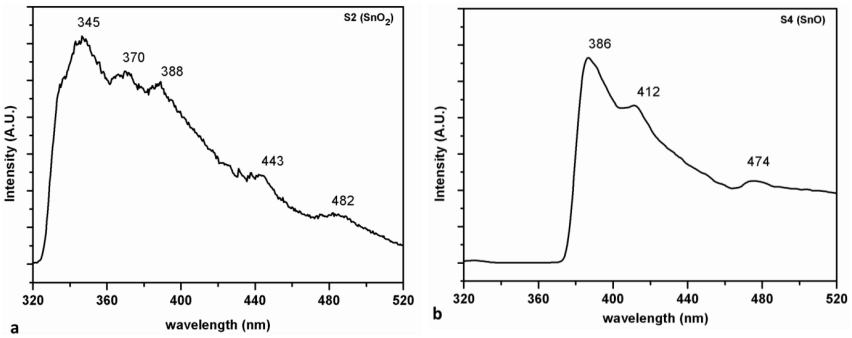

Figure 6. Photoluminescence spectra (excitation wavelength: 320 nm) for: (a) annealed S2; and (b) S4 samples.

4 Conclusions

The structural and optical properties of SnO_2 and SnO phases of tin oxide were broadly investigated and it was observed that the KOH concentration is a dominant factor for influencing the properties. Further, increase in KOH concentration found to change the phase from SnO_2 to SnO, with transformation of nanoparticle network to self-assembled microspheres. The observed increase in band gap energy is attributed to quantum size effects. The prepared sample

of SnO with 3D microstructures may show enhanced photocatalytic activity for reduction of organic pollutant.

Acknowledgements

Authors would like to acknowledge Department of Science and Technology, Gov. of India, New Delhi for financial assistance under DST-FIST scheme (SR/FST/College-258/2015, dtd.14^{th} Sep, 2016). Authors greatly acknowledge the office bearers of S. P. Sanstha, Sangamner and Principal, Sangamner College, Sangamner for encouragement and support.

References

[1] K.J. Saji, K. Tian, M. Snure, A. Tiwari (2016) 2D Tin Monoxide-An Unexplored p-Type van der Waals Semiconductor: Material Characteristics and Field Effect Transistors. *Adv. Electron. Mater*. **2** 1500453.

[2] W. Lee, Y. Liu, Y. Lee, B.K. Sharma, S.M. Shinde, S.D. Kim, K. Nan, Z. Yan, M. Han, Y. Huang, Y. Zhang, J.-H. Ahn, J.A. Rogers (2018) Two-dimensional materials in functional three-dimensional architectures with applications in photodetection and imaging. *Nat. Commun*. **9** 1417.

[3] G. von Freymann, A. Ledermann, M. Thiel, I. Staude, S. Essig, K. Busch, M. Wegener (2010) Three-Dimensional Nanostructures for Photonics. *Adv. Funct. Mater*. **20** 1038-1052.

[4] M.R. Benam, R. Hajihashemi (2014) Effect of substrate temperature on structural, optical and porosity properties of SnO2 thin films prepared by atmospheric pressure chemical vapor deposition. *Indian J. Phys*. **88** 671-675.

[5] J.S. Dias, F.R.M. Batista, R. Bacani, E.R. Triboni (2020) Structural characterization of SnO nanoparticles synthesized by the hydrothermal and microwave routes. *Sci. Rep*. **10** 9446.

[6] K.J. Saji, Y.P. Venkata Subbaiah, K. Tian, A. Tiwari (2016) P-type SnO thin films and SnO/ZnO heterostructures for all-oxide electronic and optoelectronic device applications. *Thin Solid Films*. **605** 193-201.

[7] S.A. Kuznetsova, A.A. Pichugina, V. V. Kozik (2014) Microwave synthesis of a photocatalytically active SnO-based material. *Inorg. Mater*. **50** 387-391.

[8] S. SujathaLekshmy, L.V. Maneeshya, P.V. Thomas, K. Joy (2013) Intense UV photoluminescence emission at room temperature in SnO2 thin films. *Indian J. Phys.* **87** 33-38.

[9] N. Li, Y. Fan, Y. Shi, Q. Xiang, X. Wang, J. Xu (2019) A low temperature formaldehyde gas sensor based on hierarchical SnO/SnO2 nano-flowers assembled from ultrathin nanosheets: Synthesis, sensing performance and mechanism. *Sensors Actuators B Chem*. **294** 106-115.

[10] J.A. Caraveo-Frescas, H.N. Alshareef (2013) Transparent p-type SnO nanowires with unprecedented hole mobility among oxide semiconductors. *Appl. Phys. Lett*. **103** 222103.

[11] G. Sun, F. Qi, Y. Li, N. Wu, J. Cao, S. Zhang, X. Wang, G. Yi, H. Bala, Z. Zhang (2014) Solvothermal synthesis and characterization of ultrathin SnO nanosheets. *Mater. Lett.* **118** 69-71.

[12] H. Zhang, Q. He, F. Wei, Y. Tan, Y. Jiang, G. Zheng, G. Ding, Z. Jiao (2014) Ultrathin SnO nanosheets as anode materials for rechargeable lithium-ion batteries. *Mater. Lett.* **120** 200-203.

[13] Z. Jia, L. Zhu, G. Liao, Y. Yu, Y. Tang (2004) Preparation and characterization of SnO nanowhiskers. *Solid State Commun.* **132** 79-82.

[14] B. Haspulat, M. Sarıbel, H. Kamış (2020) Surfactant assisted hydrothermal synthesis of SnO nanoparticles with enhanced photocatalytic activity. *Arab. J. Chem.* **13** 96-108.

[15] S. Arote, V. Tabhane, S. Jadkar, H. Pathan (2014) Optimization of dye loading time for SnO2 based Rose Bengal dye-sensitized solar cell. *Indian J. Phys.* **88** 1067-1071.

[16] A. Kulkarni, S. Arote, H. Pathan, M. Naushad, R. Patil (2016) Bismuth sulphide sensitized tin oxide photoelectrode for solar cell application. *Indian J. Phys.* **90** 887-893.

[17] V. Tabhane, Sandeep Arote (2018) Studies on single step facile growth of different tin oxide nanostructures at room temperature. *Indian J. Pure Appl. Phys.* **56** 7-12.

[18] J. Zhang, Y. Han, C. Liu, W. Ren, Y. Li, Q. Wang, N. Su, Y. Li, B. Ma, Y. Ma, C. Gao (2011) Electrical Transport Properties of SnO under High Pressure. *J. Phys. Chem. C.* **115** 20710-20715.

[19] L.Y. Liang, Z.M. Liu, H.T. Cao, X.Q. Pan (2010) Microstructural, Optical, and Electrical Properties of SnO Thin Films Prepared on Quartz via a Two-Step Method. *ACS Appl. Mater. Interfaces.* **2** 1060-1065.

[20] N. Ghobadi (2013) Band gap determination using absorption spectrum fitting procedure. *Int. Nano Lett.* **3** 2.

[21] A. Togo, F. Oba, I. Tanaka, K. Tatsumi (2006) First-principles calculations of native defects in tin monoxide. *Phys. Rev. B.* **74** 195128.

[22] A.M. Ganose, D.O. Scanlon (2016) Band gap and work function tailoring of SnO 2 for improved transparent conducting ability in photovoltaics. *J. Mater. Chem. C.* **4** 1467-1475.

[23] M. Aslam, T. Mahmood, A. Naeem, R. Ali (2021) Investigation of HDTMA mediated sol gel synthesis of N-doped SnO 2 nanoparticles: studies of their electrical and optical properties. *Mater. Technol.* **36** 169-178.

[24] E.J.H. Lee, C. Ribeiro, T.R. Giraldi, E. Longo, E.R. Leite, J.A. Varela (2004) Photoluminescence in quantum-confined SnO2 nanocrystals: Evidence of free exciton decay. *Appl. Phys. Lett.* **84** 1745-1747.

[25] T.W. Kim, D.U. Lee, Y.S. Yoon (2000) Microstructural, electrical, and optical properties of SnO2 nanocrystalline thin films grown on InP (100) substrates for applications as gas sensor devices. *J. Appl. Phys.* **88** 3759-3761.

[26] J. Jeong, S.-P. Choi, C.I. Chang, D.C. Shin, J.S. Park, B.-T. Lee, Y.-J. Park, H.-J. Song (2003) Photoluminescence properties of SnO2 thin films grown by thermal CVD. *Solid State Commun.* **127** 595-597.

[27] S. Sun, G. Meng, G. Zhang, T. Gao, B. Geng, L. Zhang, J. Zuo (2003) Raman scattering study of rutile SnO2 nanobelts synthesized by thermal evaporation of Sn powders. *Chem. Phys. Lett.* **376** 103-107.

[28] F. Gu, S.F. Wang, M.K. Lü, G.J. Zhou, D. Xu, D.R. Yuan (2004) Photoluminescence Properties of SnO 2 Nanoparticles Synthesized by Sol–Gel Method. *J. Phys. Chem. B*. **108** 8119-8123.

[29] B. Wang, Y.H. Yang, C.X. Wang, N.S. Xu, G.W. Yang (2005) Field emission and photoluminescence of SnO2 nanograss. *J. Appl. Phys*. **98** 124303.

[30] K. Sakaushi, Y. Oaki, H. Uchiyama, E. Hosono, H. Zhou, H. Imai (2010) Aqueous solution synthesis of SnO nanostructures with tuned optical absorption behavior and photoelectrochemical properties through morphological evolution. *Nanoscale*. **2** 2424.

[31] T. Krishnakumar, N. Pinna, K.P. Kumari, K. Perumal, R. Jayaprakash (2008) Microwave-assisted synthesis and characterization of tin oxide nanoparticles. *Mater. Lett.* **62** 3437-3440.

[32] W. Guo, L. Fu, Y. Zhang, K. Zhang, L.Y. Liang, Z.M. Liu, H.T. Cao, X.Q. Pan (2010) Microstructure, optical, and electrical properties of p-type SnO thin films. *Appl. Phys. Lett.* **96** 042113.